Oral presentation | 4 JSAP-Optica Joint Symposia 2024：4.1 Plasmonics and Nanophotonics

Mon. Sep 16, 2024 9:00 AM - 12:00 PM JST | Mon. Sep 16, 2024 12:00 AM - 3:00 AM UTC B4 (Exhibition Hall B)

[16a-B4-1~9] 4.1 Plasmonics and Nanophotonics

Prabhat Verma(Osaka Univ.)

English Presentation
9:00 AM - 9:30 AM JST | 12:00 AM - 12:30 AM UTC
[16a-B4-1]
[JSAP-Optica Joint Symposia Invited Talk] Electromagnetic Asymmetry, Quantum Conductivity and Optical Magnetism for Nonlinear Plasmonics

○Dangyuan Lei[1] (1.City Uni. of Hong Kong)

English Presentation
9:30 AM - 10:00 AM JST | 12:30 AM - 1:00 AM UTC
[16a-B4-2]
[JSAP-Optica Joint Symposia Invited Talk] Super-resolution microscopy using nonlinear behavior of fluorescent molecules

○Kenta Temma[1,2] (1.Osaka Univ. Eng., 2.Osaka Univ. Med.)

Presentation by Applicant for JSAP Young Scientists Presentation Award English Presentation
10:00 AM - 10:15 AM JST | 1:00 AM - 1:15 AM UTC
[16a-B4-3]
Anomalous Measurement of Imbert-Fedorov Shift at Surface Plasmon Resonance

○(P)CherrieMay Olaya[1], Norihiko Hayazawa[1], Maria Herminia Balgos[1], Takuo Tanaka[1] (1.RIKEN)

Presentation by Applicant for JSAP Young Scientists Presentation Award English Presentation
10:15 AM - 10:30 AM JST | 1:15 AM - 1:30 AM UTC
[16a-B4-4]
Modelling Purcell effect mediated by metasurfaces with spectral parameters

○(P)JoshuaTinYau Tse[1], Shunsuke Murai[1], Katsuhisa Tanaka[1] (1.Kyoto Univ.)

English Presentation
10:45 AM - 11:00 AM JST | 1:45 AM - 2:00 AM UTC
[16a-B4-5]
Broadband Absorption Spectroscopy via Plasmon Nanofocusing

○(M2)Haruki Kidoguchi[1], Prabhat Verma[1], Takayuki Umakoshi[1] (1.Osaka Univ.)

English Presentation
11:00 AM - 11:15 AM JST | 2:00 AM - 2:15 AM UTC
[16a-B4-6]
Suppression of Modulated Electron Beam Diffraction Radiation from Finite Array of Circular Graphene Nanotubes due to the Lattice-Mode Effect

○(P)Dariia Herasymova[1] (1.Institute of Radio-Physics and Electronics NASU)

English Presentation
11:15 AM - 11:30 AM JST | 2:15 AM - 2:30 AM UTC
[16a-B4-7]

Floquet-Mie Scattering of Time-Varying Core-Shell Nanoparticles

○(D)YUCHEN SUN[1], GUANGWEI HU[1] (1.School of Electrical and Electronic Engineering, Nanyang Technological University)

English Presentation
11:30 AM - 11:45 AM JST | 2:30 AM - 2:45 AM UTC
[16a-B4-8]

Plasmon nanofocusing vs plasmon resonance: Which generates the strongest near-field light?

○(D)Tongyao Li[1], Andrea Schirato[2,3], Remo Proietti Zaccaria[4], Prabhat Verma[1], Takayuki Umakoshi[1] (1.Osaka Univ., 2.Politecnico di Milano, 3.Rice Univ., 4.Instituto Italiano di Tecnologia)

English Presentation
11:45 AM - 12:00 PM JST | 2:45 AM - 3:00 AM UTC
[16a-B4-9]

Nanoantennas with In-plane Asymmetry for Sensing and Non-centric Emission

○Shunsuke Murai[1], Taisuke Enomoto[1], Katsuhisa Tanaka[1], Minpeng Liang[2], Jaime Gomes Rivas[2] (1.Kyoto University, 2.TU/e)

Electromagnetic Asymmetry, Quantum Conductivity and Optical Magnetism for Nonlinear Plasmonics

Dangyuan Lei
Department of Materials Science and Engineering, City University of Hong Kong, Hong Kong
E-mail: dangylei@cityu.edu.hk

In general, symmetric plasmonic nanocavities, such as a pair of two closely spaced metal nanospheres of the same size and constituting material, support only symmetry-allowed bright modes under light illumination. Breaking the cavity symmetry introduces mode hybridization between its bright and dark modes, leading to new plasmon modes like Fano resonance and bound states in the continuum.

In this talk, I will go on to discuss three "dark" aspects of symmetry-broken plasmonic nanocavities, including 1) light-induced electromagnetic asymmetry for enhancing the surface second-harmonic generation (SHG) of noble metals (**Nature Communications 2021, 12, 4326**), a mechanism well beyond conventional enhancement strategies, 2) photon-assisted tunnelling induced second-order nonlinear optics in conductive molecular nano-junctions (**Nano Letters 2023, 23(12), 5851-5858**), and 3) plasmon-induced optical magnetism in an asymmetric nanoparticle dimer-on-mirror cavity and its theoretical implication as a new second-order nonlinear source (**Laser & Photonics Reviews 2020, 14(9), 200068**).

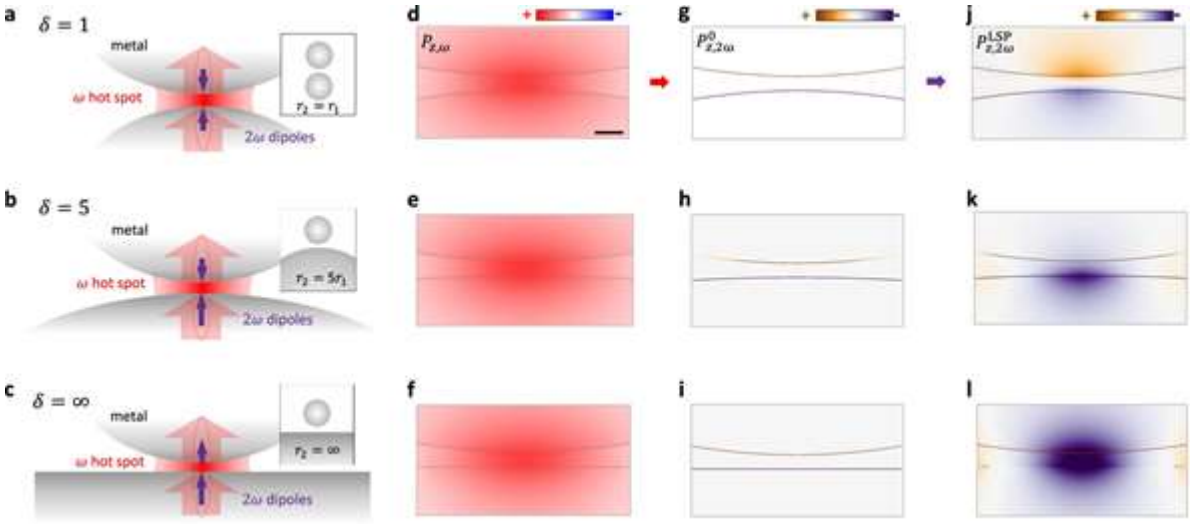

Figure 1: Suppressed and amplified surface second-harmonic generation in symmetric (upper panel) and asymmetric (middle and lower panels) plasmonic nanocavities

Short Bio:

Dangyuan LEI received his PhD degree in Physics from Imperial College London, UK. He is Professor of Materials Science and Engineering at The City University of Hong Kong, China, and Provost's Visiting Professor of Physics at Imperial College London. His research interest centres on nanophotonics and low-dimensional quantum materials, with particular interest in the nanoscale cavity-matter interaction.

Super-resolution microscopy using the nonlinear behavior of fluorescent molecules

Dept. of Applied Physics, Osaka Univ. [1], Dept. of Neurosurgery. Osaka Univ. [2],

Kenta Temma[1, 2]

E-mail: temma@ap.eng.osaka-u.ac.jp

Fluorescence microscopy is an indispensable tool for observing biological samples due to its less invasiveness, target specificity, and single-molecule sensitivity. The development of super-resolution techniques such as stimulated emission depletion (STED) [1], single-molecule localization [2], and structured illumination microscopy (SIM) [3] have overcome the limitation in spatial resolution, expanding the capability for imaging with higher spatial resolution beyond the classical diffraction limit. However, most of the super-resolution techniques fully exhibit their resolving capability only near the surface of samples, due to the requirement of complex illumination patterns or single molecule detection. These techniques are often hampered by background light from out-of-focus or optical aberrations, making the observation of internal structure difficult, especially in thick samples.

We developed several super-resolution techniques that leverage the nonlinear behavior of fluorescent molecules such as multiphoton [4], saturable [5], and step-wise absorption [6,7]. Nonlinear fluorescence signals derived from these behaviors are three-dimensionally localized within the excitation area, suppressing background light and improving the spatial resolution even within thick samples.

In this talk, I will introduce our development of super-resolution techniques using reversibly photo-switchable fluorescent proteins (RSFPs) whose capability of fluorescence emission (off and on state) can be modulated by light irradiation. We combined the nonlinear property of RSFPs and two-photon excitation to induce higher-order nonlinear response for further improvement of spatial resolution [6]. We also utilized RSFPs to integrate two illumination patterns: selective plane illumination and structured illumination [7]. Localizing fluorescent regions through selective plane activation of RSFPs enables the use of SIM in thick samples by suppressing background light. We succeeded in observing the internal structure of a single cell and large cell clusters with high spatial resolution, which was a difficult task for conventional super-resolution microscopy.

References

[1] S. W. Hell and J. Wichmann, *Opt. Lett.* **19**, 780-782 (1994)

[2] E. Betzig et al., *Science*, **313**, 1642-1645 (2006)

[3] M. G. L. Gustafsson, *J. Microsc.,* **198**, 82-87 (2000)

[4] T. Kubo, K. Temma et al., *Opt. Lett.,* **46**, 37-40 (2021)

[5] T. Kubo, K. Temma et al., *ACS Photonics,* **8**, 2666-2673 (2021)

[6] K. Temma et al., *Opt. Express,* **30**, 13825-13838 (2022)

[7] K. Temma and R. Oketani, et al, *Nat. Methods*, **21**, 889-896 (2024)

Anomalous Measurement of Imbert-Fedorov Shift at Surface Plasmon Resonance

Cherrie May Olaya[1], Norihiko Hayazawa[1,2], Maria Herminia Balgos[1], Takuo Tanaka[1,3]

[1] Innovative Photon Manipulation Research Team, RIKEN Center for Advanced Photonics, Japan,
[2] Surface and Interface Science Laboratory, RIKEN Cluster for Pioneering Research, Japan
[3] Metamaterials Laboratory, RIKEN Cluster for Pioneering Research, Japan
E-mail: cherriemay.olaya@riken.jp

1. Introduction

The interaction of a real optical beam and a planar interface results in an apparent shift of the reflected beam with respect to the prediction of geometric optics. The reflected beam could be displaced along the optical axis, called Goos-Hänchen (GH) shift, or transverse to the optical axis, called Imbert-Fedorov (IF) shift [1,2]. GH shift arises from the diffraction corrections in the reflection coefficients while IF shift originates from the spin-orbit (SOI) interaction of photons due to the conservation of total angular momentum. IF shifts are typically observed under circularly polarized source or under 45° linearly polarized source which correspond to the eigenmode of the shift [3]. As such, upon excitation of surface plasmon resonance under p-polarized illumination, GH shifts occurs whereas no IF shift is expected. In our previous works [4-6] and elucidated during the 2020 JSAP Autumn Meeting [7], we demonstrated significant enhancement of GH shifts at the SPR region that agree well with theoretical calculations. In this work, however, we show a large anomalous IF shift measured at the SPR angle.

2. Methodology

Modifications to the experimental system used in our previous works in [4-6] allowed for the simultaneous measurements of GH and IF shifts around the SPR region. Thin film of gold (t_{Au} = 47. 5 nm) with titanium (t_{Ti} = 2.5 nm) adhesion layer was used as substrate. Excitation of surface plasmons were made using the standard Kretschmann configuration where a linearly polarized laser diode (λ = 633 nm) impinges the substrate through a hemispherical prism (ϕ = 25 mm). The polarization state of the incident beam is switched between p and s states using an electro-optic (EO) modulator. Reflected beam centroid displacements were obtained using a quadrant detector (QD) positioned 4.5 cm from the incident beam waist.

3. Results and Discussion

Fig. 1 shows the GH and IF shifts measured around the SPR region. The gray line shows the location of the SPR angle which was obtained from reflectivity measurements performed simultaneously with beam shift measurements. The measured GH shift agrees well with analytical calculations where an angular GH shift-dominated is shown for a focused incident beam.

Analytically, no IF shift should be measured since IF shift does not have an eigenmode at p and s polarization state. Our measurements, however, show otherwise where a sharp

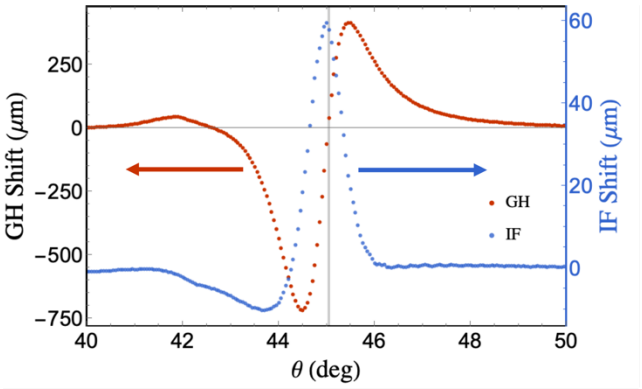

Figure 1. GH (red) and IF (blue) shift of the reflected beam. The gray line corresponds to the location of the SPR angle.

IF shift is measured at the SPR angle as shown in blue dots in Fig. 1. We surmise that the sharp IF shift arises from the polarization mixing from the focused incident beam and the finite extinction of the EO modulator, where for a focused incident beam, any slight deviation from the pure polarization state would result to large IF shifts. We deem our results essential to measurements requiring high precision especially for microscopy-based setups where high numerical aperture lenses are used.

3. Conclusions

We measured significantly large beam shifts along and perpendicular to the optical axis upon excitation of surface plasmon resonance. While the in-plane GH shift agrees well with analytical calculation, we measured significantly large anomalous IF shift at the SPR angle which we surmise to have originated from the polarization mixing of the focused incident beam.

References

[1] K. Y. Bliokh, A. Aiello, J. Opt. **15** (2013) 014001.
[2] C. F. Li Phys. Rev. A. **76** (207) 013811.
[3] K. Y. Bliokh, F. J. Rodríguez-Fortuño, F. Nori, and A. V. Zayats, Nat. Photonics **9**, 796–808 (2015).
[4] C. Olaya, N. Hayazawa, N. Hermosa, T. Tanaka, J. Phys. Chem. A, 2021, **1**, 451-458.
[5] C. Olaya, N. Hayazawa, M. Balois-Oguchi, N. Hermosa, T. Tanaka, Sensors, 2021, **21**, 13, 4593.
[6] C. Olaya, N. Hayazawa, M. Balgos, T. Tanaka, Appl. Opt., 2023, **62**, 8426-8433.
[7] C. Olaya, N. Hayazawa, N. Hermosa, T. Tanaka, in JSAP-OSA Joint Symposia, 2020.

Modelling Purcell effect mediated by metasurfaces with spectral parameters

Joshua Tin Yau Tse[1], Shunsuke Murai[1], Katsuhisa Tanaka[1]

[1] Department of Material Chemistry, Graduate School of Engineering, Kyoto University
E-mail: tse@dipole7.kuic.kyoto-u.ac.jp

1. Introduction

Empirically measuring the Purcell factor, which represents the maximum enhancement to spontaneous emission in an optical cavity, is straightforward as the photoluminescence enhancement (PLE) can be determined directly by comparing the luminescence intensity with and without the cavity. However, predicting the Purcell factor have been proven to be tricky. In particular, the effective modal volume is difficult to analyze empirically, especially for non-Hermitian systems which includes open resonators and systems with dissipative materials [1].

Surface lattice resonances (SLR) is a hybrid plasmonic-photonic resonance supported on nanoparticle arrays that provides strong and directional PLE via Purcell effect and directional out-coupling. In this work, we analyzed the Purcell effect arising from SLR and proposed an analytical model that predicts the PLE only with parameters that can be obtained through spectral measurements. We also studied a wide variety of structures to ensure the predictive power of the model.

2. Analytical Model

In our recent work that explores the effectiveness of different materials used in PLE [2], we discovered that the nearfield enhancement of SLR in the embedded dye layer can be mapped to the absorptive decay rate contributed by dye $\Gamma_{abs,dye}$, which is a parameter that is obtained through spectral measurement and fitting. Through the Lorentz reciprocity theorem, we also learned that the nearfield enhancement is a predictor of PLE that is commonly used in numerical analysis [3]. By connecting these insights, we derived a new method in determining the Purcell factor of SLR that only uses parameters that can be obtained from spectral measurements. In particular, we find the spontaneous emission enhancement provided by the SLR to be described by:

$$PLE(\omega_0) = \frac{c\Gamma_{rad}}{\omega_0 t \Gamma_{tot}^{\,2}} \frac{\Gamma_{abs,dye}}{\kappa}$$

where ω_0 is the resonant frequency, Γ_{rad} is the radiative decay rate of the SLR, t is the dye layer thickness, κ is the extinction coefficient of the dye layer, and c is the speed of light in vacuum. Γ_{tot} is the total decay rate and $\Gamma_{tot} = \Gamma_{rad} + \Gamma_{abs,dye} + \Gamma_{abs,NP}$, where $\Gamma_{abs,NP}$ is the absorptive decay rate contributed by the nanoparticles.

3. Results and Discussion

In order to verify our analytical model, we numerically simulated SLRs on nanoparticle arrays of different materials and geometries with the finite-difference time-domain (FDTD) method. The numerically simulated PLE of each structure are plotted against the PLE predicted by our analytical model in Figure 1 for comparison. As illustrated in Figure 1, the data closely follows the diagonal line, which indicates that our model predicted the PLE in numerous simulated structures.

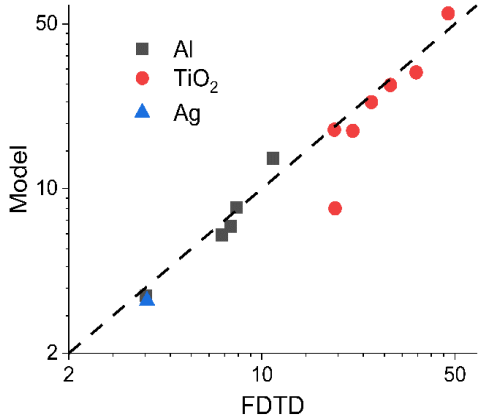

Figure 1. The PLE predicted by the analytical model was plotted against the FDTD simulated PLE.

We also experimentally analyzed PLE measurements with TiO_2 nanoparticle arrays. The experimental results verified the predictions from our analytical model. We also discovered that some parameters can be generalized over multiple structures with similar features. This insight allows us to further extend the predicting power of our analytical model with limited information.

4. Conclusions

In conclusion, we developed an analytical model that describes the Purcell effect using Lorentz reciprocity theorem. With our analytical model, we predicted the PLE mediated by SLRs on multiple structures made of a variety of materials in both numerical simulations and experiments. This study presents a useful analytical framework for optimizing PLE on a wide variety of plasmonics and nanophotonics resonators.

References

[1] C. Sauvan, J. P. Hugonin, I. S. Maksymov, and P. Lalanne, Phys. Rev. Lett. **110** (2013), 237401.
[2] J. T. Y. Tse, S. Murai, and K. Tanaka, Adv. Photonics Res. (2024), 2400050.
[3] M. Ramezani, G. Lozano, M. A. Verschuuren, and J. Gómez-Rivas, Phys. Rev. B **94** (2016), 125406

Broadband Absorption Spectroscopy via Plasmon Nanofocusing

Haruki Kidoguchi[1], Prabhat Verma[1], Takayuki Umakoshi[1,2]

[1]Dept. of Applied Physics, Osaka University, [2] Inst. Adv. Co-creation Studies, Osaka University
E-mail: umakoshi@ap.eng.osaka-u.ac.jp

1. Introduction

Plasmon nanofocusing is a phenomenon that generates strong near-field light at an apex of a metallic tapered structure through plasmon propagation and focusing toward the apex. Among its various characteristics such as background-free from incident light, one of its distinctive advantages is the broadband property. Unlike localized plasmon resonance of a metallic nanostructure, which is excited only near the plasmon resonance wavelength, plasmon nanofocusing is excited over an extremely broad wavelength range as it is not based on resonance, but propagation of plasmons. As we have previously demonstrated the generation of white nanolight source through plasmon nanofocusing for optical nanoimaging [1], broadband plasmon nanofocusing holds a great potential for various nanophotonics techniques.

In this study, we applied plasmon nanofocusing for broadband absorption spectroscopy. Absorption spectroscopy has been a fundamental analytical technique for various samples. The previous study has further demonstrated the highly sensitive absorption sensing based on the localized surface plasmon resonance [2]. However, this resonance-based approach is limited in its detection wavelength range, which makes it difficult to precisely analyze absorption spectral shape or to simultaneously detect multiple different peaks. To overcome this issue, we employed broadband plasmon nanofocusing, and experimentally demonstrated broadband absorption spectroscopy.

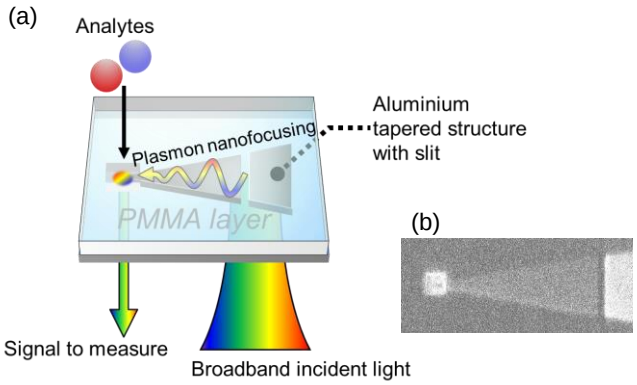

Fig. 1 (a) Schematic of our method. (b) SIM image of the tapered metallic structure (after deposition of the protection layer).

2. Results and Discussion

To demonstrate broadband absorption spectroscopy based on plasmon nanofocusing, we used the setup summarized in Fig. 1a. The aluminium tapered structure was fabricated by first depositing an aluminium thin film via vacuum evaporation and then patterning it using a focused ion beam (FIB). A slit structure was fabricated as a plasmon coupler. Subsequently, the entire tapered structure was covered with a PMMA thin film as a protection layer, and a detection hole was fabricated near the apex using FIB so that only the apex was exposed to detect absorption at the tip of the tapered structure (Fig.1b). The white supercontinuum laser was shined on the plasmon coupler to excite plasmons. Propagating plasmons generate a white nanolight source at the apex, which was used for the broadband absorption spectroscopy.

For absorption measurement, a water drop was first deposited on the substrate, and analytes solution was subsequently injected for measurements. Absorption spectra were calculated by comparing the scattering signals from the taper apex with analytes and without analytes. As shown in Fig. 2, we successfully acquired absorption spectra of three different analytes Cy3, Cy5 and Cy7.5 simultaneously, which have different absorption peaks from 500 to 800 nm over a broad wavelength range. The result was in a good agreement with the spectrum obtained with the conventional absorption spectrometer. Also, we confirmed that our method has a linearity despite the limited detection sensitivity due to the mechanical drift of optical components at this moment.

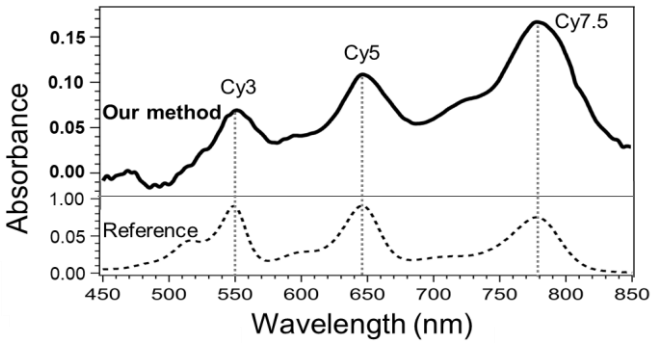

Fig. 2 Absorption spectrum acquired via plasmon nanofocusing (solid line) and reference spectrum by conventional spectrometer (dashed line).

3. Conclusion

We successfully demonstrated broadband absorption spectroscopy based on plasmon nanofocusing ranging from 500 nm to 850 nm.

References

[1] T. Umakoshi, et al. *Sci. Adv.* **6**, eaba4179 (2020).
[2] Liu, G. et al. *Nat. Methods.* **4**, 1015–1017 (2007).

Suppression of Modulated Electron Beam Diffraction Radiation from Finite Array of Circular Graphene Nanotubes due to the Lattice-Mode Effect

Dariia O. Herasymova

Laboratory of Micro and Nano Optics, Institute of Radio-Physics and Electronics NASU, Kharkiv 61085, Ukraine
E-mail: dariia.heras@gmail.com

We analyze the effect of the suppression of the diffraction radiation (DR) caused by the electron beam flowing above a finite grating made of dielectric circular nanowires with graphene covers – see Fig.1. The work focuses on the combined effect of the plasmon-mode and the lattice-mode resonances on DR.

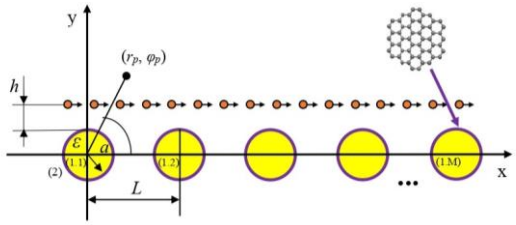

Fig. 1. Cross-sectional geometry of flat zero-thickness electron beam moving near *M* identical circular dielectric nanowires.

In our analysis, we assume that the zero-thickness electron beam density is time-harmonically modulated with the cyclic frequency ω and its velocity is constant, $v = \beta c$, and consider its field in the free space as the incident field [1-4]. To characterize the graphene, we employ the quantum-theory Kubo formalism and the resistive sheet boundary conditions [5]. Then, the DR problem is a full-wave two-dimensional boundary-value problem for the Helmholtz equation with exact boundary conditions, plus the condition of local power finiteness and the radiation condition at infinity. To cast this problem to the form convenient for computations, we use the separation of variables in local coordinates and the addition theorem for cylindrical functions that yields a block type (*M* x *M*) infinite-matrix equation of the Fredholm second kind. This enables precise control of numerical accuracy [4]. The DR power characteristics, such as the total scattering cross-section, are calculated.

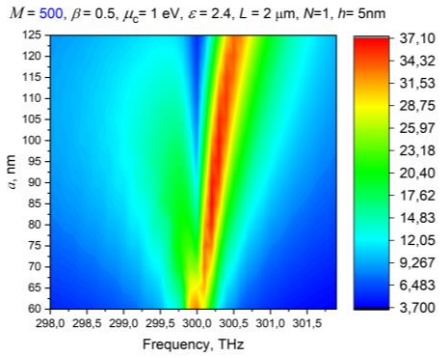

Fig. 2. Color map of the DR power versus the frequency and the wire radius for the *M* = 500 graphene-wrapped nanowire grating.

Fig. 2 shows the color map of the DR total scattering cross-section (TSCS) for the electron beam excited grating of *M* = 500 wires with the radius varying from 60 nm to 125 nm near the 300 THz frequency. The chemical potential of graphene is 1 eV, and the electron beam relative velocity is β = 0.5. The red "ridge" on the map, visible for the wires of all radii, corresponds to the resonance on the dipole plasmon mode P_1 of the graphene cover of each nanowire. The Q-factor of that resonance is moderate, around 53 according to equation (26) from [4]. Our previous works [6] have revealed that such a grating with the number of wires that is counted in large dozens and hundreds possesses an ultrahigh-Q lattice-mode resonance [7,8] at the frequency where period is entirely divisible by wavelength/β. If the frequencies of the plasmon and lattice mode resonances are well separated, each of them yields a peak in the DR power spectrum. In the studied here case of the 2-μm period, the mentioned two resonance frequencies coincide. As one can observe from Fig. 2, then the collective lattice-mode effect is not distinguished if the wire radius is smaller than around 90 nm. However, if it gets larger, then there happens a suppression of the plasmon-mode resonance peak – TSCS has a deep minimum. The larger the wire radius, the deeper the suppression. The potential application of the studied effects is discussed.

References:

[1] A. I. Boltonosov and V. G. Sologub, "Excitation of an open strip-type resonator by a modulated beam of charged particles," Sov. J. Communic. Technol. Electron., vol. 33, no 6, pp. 133-140, 1988.
[2] M. Castellano, et al., "Measurements of coherent diffraction radiation and its application for bunch length diagnostics in particle accelerators," Phys. Rev. E, vol. 63, art. no 056501, 2001.
[3] D. Assante, et al., "Longitudinal coupling impedance of a particle traveling in PEC rings: A regularised analysis," IET Microwaves, Antennas Propag., vol. 15, no 10, pp. 1318–1329, 2021.
[4] D. O. Herasymova, S. V. Dukhopelnykov, and A. I. Nosich, "Infrared diffraction radiation from twin circular dielectric rods covered with graphene: plasmon resonances and beam position sensing," J. Opt. Soc. Am. B, vol. 38, no 9, pp. C183-C190, 2021.
[5] G. W. Hanson, "Dyadic Green's functions and guided surface waves for a surface conductivity model of graphene," J. Appl. Phys., vol. 103, art. no 064302, 2008.
[6] D. O. Herasymova, "Diffraction radiation analysis of finite graphene-covered nanowire grating excited by electron beam," Proc. European Microwave Conf. (EuMC-2023), Berlin, 2023, pp. 544-547.
[7] V. O. Byelobrov, T. L. Zinenko, K. Kobayashi, et al., "Periodicity matters: grating or lattice resonances in the scattering by sparse arrays of sub-wavelength strips and wires," IEEE Antennas Propag. Mag., vol. 57, no 6, pp. 34-45, 2015.
[8] A. D. Utyushev, et al., "Collective lattice resonances: plasmonics and beyond," Rev. Phys., vol. 6, art. no 100051, 2021.

Floquet-Mie Scattering of Time-Varying Core-Shell Nanoparticles

Yuchen Sun[1], Guangwei Hu[1]

[1] School of Electrical and Electronic Engineering, 50 Nanyang Avenue, Nanyang Technological University, Singapore, 639798, Singapore
E-mail: guangwei.hu@ntu.edu.sg

1. Introduction

Extreme scattering phenomena, such as nonreciprocity, and parametric amplification, in periodically time-varying mediums have attracted numerous attentions in recent years. Periodically time-varying permittivity is used as an additional degree of freedom in metamaterials or metasurfaces. Here, we investigate the Floquet Mie scattering properties of a spherical nanoparticle coated with a time-varying dispersive shell. Our result can provide insight into the light-matter interaction in the time-varying system and can also guide the antenna design based on the core-shell structure.

2. General Instructions

We consider a circularly polarized light impinges on a temporal modulated spherical core-shell nanoparticle. The spherical particle consists of a dielectric core with radius a and a time-varying dispersive shell with radius b. The electric field inside the shell can be expanded as a series of vector spherical harmonics (VSFs) $\mathbf{F}(\kappa\mathbf{r})$,

$$\mathbf{E}(\mathbf{r},\omega)=\sum_{\kappa}A(\kappa)S_{\kappa}(\omega)\mathbf{F}(\kappa\mathbf{r}),$$

where κ is the wavenumber, $S_{\kappa}(\omega)$ is the spectral part of the eigenmode.

Dispersion relation inside the periodically time-varying dispersive material

We consider the plasmonic materials with periodically modulated electron density, which can be realized via "shaking" the metal with pulse etc. The electron motion can be described by the equation of motion [1,2],

$$\left[\frac{\partial^2}{\partial t^2}+\gamma\frac{\partial}{\partial t}+\omega_r^{\,2}\right]\mathbf{P}(\mathbf{r},t)=\frac{q_e^{\,2}}{m_e}N(t)\mathbf{E}(\mathbf{r},t)$$

where $N(t)=N_0(1+\Delta\cos\Omega t)$. And the permittivity can be solved from this equation. After substituting the permittivity into the Maxwell's equations, the dispersion relation takes this form,

$$k(\omega)^2\left(\varepsilon_{st}(\omega)S_{\kappa}(\omega)+\varepsilon_{dyn}(\omega)S_{\kappa}(\omega+\Omega)+\varepsilon_{dyn}(\omega)S_{\kappa}(\omega-\Omega)\right)=\kappa^2S_{\kappa}(\omega)$$

where $\varepsilon_{st}=1+\dfrac{\omega_p^2}{\omega_r^{\,2}-\omega^2-i\gamma\omega},\varepsilon_{dyn}=\dfrac{\Delta}{2}\dfrac{\omega_p^2}{\omega_r^{\,2}-\omega^2-i\gamma\omega}$

The results

The electromagnetic field inside the time-varying shell can be written as,

$$\mathbf{E}_{shell}(\mathbf{r},\omega)=\sum_{\alpha,\mu\nu}\sum_{i=-\infty}^{\infty}\sum_{n=-\infty}^{\infty}\sum_{j=1,2}S_{\kappa_i}(\omega-n\Omega)A^{(j),shell}_{\alpha,\mu\nu,\kappa_i}\mathbf{F}^{(j)}_{\alpha,\mu\nu,\kappa_i}(\mathbf{r})$$
$$\mathbf{H}_{shell}(\mathbf{r},\omega)=\sum_{\alpha,\mu\nu}\sum_{i=-N}^{N}\sum_{n=-N}^{N}\sum_{j=1,2}B^{(j),shell}_{\alpha,\mu\nu,\kappa_i}\mathbf{F}^{(j)}_{\alpha,\mu\nu,\kappa_i}(\mathbf{r})$$

Applying the boundary conditions, i. e., the continuity of the tangential component of electric and magnetic field, the scattered field can be solved.

We calculate its elastic scattering cross section using the scattered field. As is shown in Figure 1, the elastic scattering cross section is strongly suppressed at the resonance frequency.

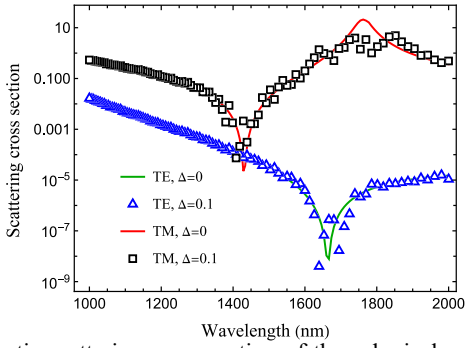

Figure 1. Elastic scattering cross section of the spherical particle with core-shell structure. [3] Their radius is set as $a=100\ nm$ and $b=150\ nm$, the modulation strength $\Delta=0$ and 1, and modulation frequency $\Omega=0.377$ THz.

3. Conclusions

We have proposed a rigorous method to describe the scattering properties of the spherical particle with a time-varying dispersive shell. We calculated the scattering cross section. The results may help us understand the energy transfer between the EM field and the time-varying medium.

References

[1] I. Stefanou, J. Opt. Soc. Am. B **38** (2021) 407.

[2] G. Ptitcyn, Laser Photon. Rev. **17** (2022) 2100683.

[3] F. Monticone, Phys. Rev. Lett. **110** (2013) 113901.

Plasmon nanofocusing vs plasmon resonance: Which generates the strongest near-field light?

Tongyao Li[1], Andrea Schirato[2,3], Remo Proietti Zaccaria[4], Prabhat Verma[1], Takayuki Umakoshi[1,5]

[1]Dept. of Applied Physics, Osaka Univ., [2]Physics Dept., Politecnico di Milano, [3]Dept. of Physics and Astronomy, Rice University, [4]Instituto Italiano di Tecnologia, [5]Institute of Advanced Co-Creation Studies, Osaka Univ.,
E-mail: umakoshi@ap.eng.osaka-u.ac.jp

1. Introduction

Strongly localized and enhanced near-field light generated near plasmonic nanostructures has been widely applied in various fields from material science to biology. The near-field light is often generated by localized plasmon resonance of metallic nanostructures such as a gold nanoparticle and nanorod. Recently, plasmon nanofocusing has also attracted much attention as another method to generate the near-field light due to its distinctive advantages such as background-free from incident light [1]. The near-field light is generated at an apex of a plasmonic tapered structure, such as a gold cone, through plasmons propagating toward the apex. Considering both methods of localized plasmon resonance and plasmon nanofocusing, one of pivotal questions is “Which generates more intense near-field light?”, as the near-field light intensity is a fundamental and important property for most of optical applications.

2. Results and discussion

In this study, we numerically investigated which of localized plasmon resonance and plasmon nanofocusing generates intense near-field light. To evaluate the maximum near-field light intensities for both methods, we considered not only light field intensity but also heat generation and temperature in plasmonic structures. The near-field light intensity can be simply increased by increasing the incident light intensity. However, it is limited by the fact that too strong incident light destroys plasmonic structures as temperature goes beyond the melting point. Therefore, we calculated both electric field and temperature around the plasmonic structures using finite element method.

Figure 1(a) shows the calculation models for the localized plasmon resonance and plasmon nanofocusing. We chose 785 nm as the incident light wavelength. We used a gold nanorod and cone for the localized plasmon resonance and plasmon nanofocusing, respectively, as typical structures. Their geometries were optimized for the wavelength of 785 nm. We used a grating as a plasmon coupler for plasmon nanofocusing, which was located 3.75 μm far from the apex. Under incident light irradiation to the gold nanorod and the grating of the gold cone, we simulated the distributions of both the electric field and temperature, as shown in Figs. 1 (b, c). We confirmed that near-field light was generated for both cases. At the same time, we found that temperature of the structures increased due to heat generation. We further increased incident light intensity

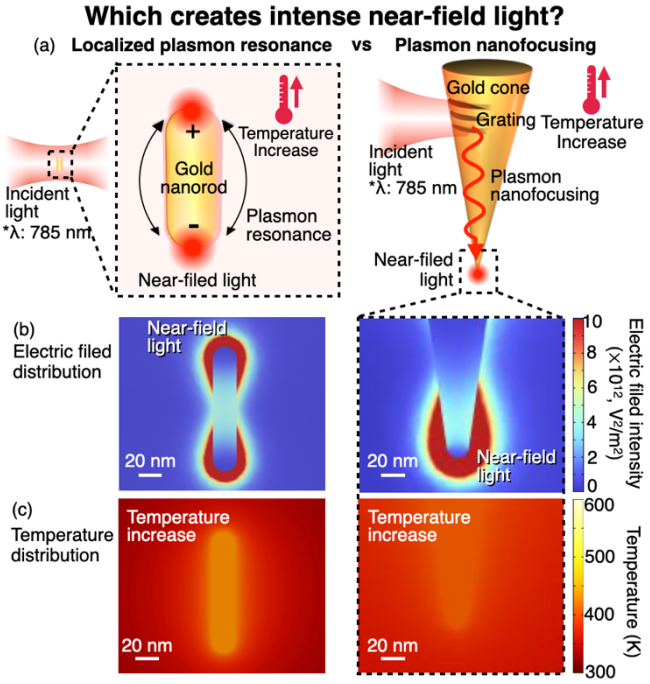

Figure 1 Fig 1. (a) Schematics of calculation modes of (b) Electric field and (c) temperature distributions of the gold nanorod and cone.

until temperature reaches the melting point of gold (1337K). In this situation, we found that the maximum near-field light intensity by plasmon resonance was 6.26×10^{13} V^2/m^2. As for plasmon nanofocusing with the gold cone, the maximum near-field light intensity was 11.40×10^{13} V^2/m^2. Therefore, we concluded that plasmon nanofocusing is capable of creating approximately twice stronger near-field light compared with localized plasmon resonance.

3. Conclusions

In conclusion, we found that plasmon nanofocusing generates twice more intense near-field light compared with localized plasmon resonance. However, it was investigated only at a particular condition, which calls more extensive studies at various conditions in the future. In the presentation, we also discuss the case of more moderate temperature. Also, an interesting phenomenon of the near-field light intensity decrease with respect to the incident light intensity will be discussed.

References

[1] T. Umakoshi, et al., *Sci. Adv.* **6**, eaba4197 (2020)

Nanoantennas with In-plane Asymmetry for Sensing and Non-centric Emission

Shusuke Murai[1], Taisuke Enomoto[1], Katsuhisa Tanaka[1], Minpeng Liang[2], Jaime Gómez Rivas[2]

[1] The Japan Society of Applied Physics, Department of Material Chemistry, Graduate School of Engineering, Kyoto University [2] Department of Applied Physics and Science Education, Institute for Complex Molecular Systems, and Eindhoven Hendrik Casimir Institute, Eindhoven University of Technology, The Netherlands
E-mail: murai.shunsuke.2m@kyoto-u.ac.jp

1. Introduction

When light is incident on a nanoantenna, i.e., a periodic array of nanoparticles, individual local resonances couple cooperatively and produce surface lattice resonance (SLR). Operating the in-plane symmetry of the nanoantenna would break the in-plane symmetry of the optical response of the SLRs, and also lead to the suppression of radiation of the SLRs to become bound-states in the continuum (BICs) [1]

In this study, we prepared two samples with in-plane asymmetry: the first sample is the square lattice comprising asymmetric-shaped TiO_2 nanoparticles. The second sample is non-Bravais lattice of Si nanoparticles array, supporting quasi-BIC states at normal incidence. Using these asymmetric nanoantennas, we investigated non-centric directional photoluminescence and sensitivity to the surrounding refractive index.

2. Asymmetric TiO_2 nanoantenna for non-centric emission

The asymmetric TiO_2 nanoparticle arrays were fabricated by a glancing angle deposition of titanium on the square lattice of TiO_2 nanoparticle array at an angle of 45° to the substrate, followed by rapid thermal annealing (RTA) to convert the deposited Ti to TiO_2. The shape of the nanoparticle was observed by scanning electron microscopy (SEM) and atomic force microscopy. In the SEM image (Fig. 1(a)), a shadow can be seen on the right side of each nanoparticle, indicating that the titanium was deposited from the left side.

We measured the incident angle dependence of the extinction spectra of the poly(methyl methacrylate) (PMMA)-coated array on the substrate (Fig. 1(b)) and the emission angle dependence of the PL enhancement of the PMMA-coated array containing a fluorescent dye (Fig. 1(c)) along the *x*-axis. In the extinction spectra, two dispersive features are found along the (±1,0) diffraction orders. Their intensities are very different because of the asymmetric shape of the nanoparticles. The PL enhancement map (in Fig. 1(c) follows this asymmetric intensity. These results show that the simple glancing angle deposition makes the asymmetric nanoparticle arrays to shift the center of the luminescence intensity distribution.

3. Doubly-detuned Si nanoantenna for sensing

We broke the in-symmetry by detuning the size and position of silicon particles periodically arranged in an array, resulting in magnetic and electric quasi-BICs at gamma point. We investigated the sensing characteristics of them by measuring the spectral shift in response to changes in the refractive index of the surrounding medium[2]. In addition, we revealed the sensing range of the different resonances through simulations involving a layer of deviating refractive index of increasing thickness. Interestingly, the resonances show very different responses, which we describe via the analysis of the near-field. This work contributes to the development of highly sensitive and selective BIC-based sensors that can be used for a wide range of applications.

Acknowledgements

Financial support from JSPS bilaterial Joint Research Project (JPJSBP120239921) was acknowledged.

References

[1] S. Murai et al., Laser Photon. Rev. 2100661 (2022)
[2] T. van Loon et al. Optics Express 32, 14289-1429 (2024)

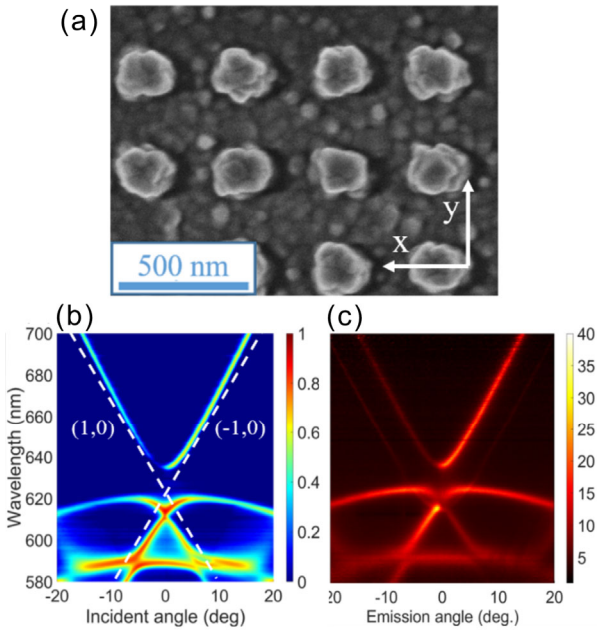

Fig.1(a) SEM image of asymmetric TiO_2 nanoparticle arrays prepared with glancing angle deposition. Angular dependent (b) extinction and (c) photoluminescence enhancement (PLE) spectra of the asymmetric TiO_2 nanoparticles arrays. The dotted lines in (b) denote (±1,0) diffraction orders. PLE was defined as the PL intensity from the luminous layer on the array divided by that from the same layer but on a flat substrate.